



**HAL**  
open science

## Does winter come? Predicting endodormancy induction in walnut trees.

Guillaume Charrier

► **To cite this version:**

Guillaume Charrier. Does winter come? Predicting endodormancy induction in walnut trees.. 2021.  
hal-03065757v3

**HAL Id: hal-03065757**

**<https://hal.inrae.fr/hal-03065757v3>**

Preprint submitted on 24 Nov 2021

**HAL** is a multi-disciplinary open access archive for the deposit and dissemination of scientific research documents, whether they are published or not. The documents may come from teaching and research institutions in France or abroad, or from public or private research centers.

L'archive ouverte pluridisciplinaire **HAL**, est destinée au dépôt et à la diffusion de documents scientifiques de niveau recherche, publiés ou non, émanant des établissements d'enseignement et de recherche français ou étrangers, des laboratoires publics ou privés.

1 **Does winter come? Predicting endodormancy induction in walnut trees.**

2

3 **Running title: Predicting endodormancy induction in walnut trees**

4

5 Guillaume Charrier<sup>1</sup>

6 <sup>1</sup>**Université Clermont Auvergne, INRAE, PIAF, 63000 Clermont-Ferrand, France**

7 \*: corresponding author

8 Email: [guillaume.charrier@inrae.fr](mailto:guillaume.charrier@inrae.fr)

9 Tel: +33 4 43 76 14 21

10 UMR PIAF, INRAE Site de Crouel

11 5, chemin de Beaulieu

12 63000 Clermont-Ferrand

13

14 **Abstract**

15 The initial date for chilling accumulation ( $D_{CA}$ ) is often set arbitrarily using various rules and  
16 leading to a tremendous variability between studies and sites. To test the relevancy of different  
17 calculation rules, sequential models taking into account, or not, the negative effect of warm  
18 temperature) were optimized on 34 endodormancy release and 77 budbreak dates of walnut cv  
19 Franquette across France. The flexible  $D_{CA}$  was more efficient than using functions that  
20 compute negative chilling accumulation at warm temperature. Most of the  $D_{CA}$  tested provided  
21 an accurate fit to the calibration datasets for budbreak, but less for endodormancy release.  
22 Among the rules, the DORMPHOT model, integrating temperature and photoperiod control on  
23 endodormancy induction, was the most efficient (RMSEP < 10 and 8 days for endodormancy  
24 release and budburst, respectively). The projections of the best model under different climate  
25 (current and RCP *scenarii*) revealed a tipping point at a mean annual temperature of 13.86°C,  
26 beyond which the advance in ontogenic development during endodormancy does not compensate  
27 the delay in endodormancy release. The relationships between climate variables and plant  
28 phenological processes would help to predict future phenological cycles on a global scale.

29 **Keywords:** Budburst, Chilling, Dormancy induction, Endodormancy release, Forcing, *Juglans*  
30 *regia* L, Photoperiod, Phenology, Trees.

## 31 **Introduction**

32 In frost-exposed environments, deciduous trees have to timely adjust their phenology to  
33 anticipate unfavorable conditions during the winter period. To avoid exposure to frost events,  
34 meristems switch from an apparently active period to a ‘dormant’ period, characterized by the  
35 inability to grow even under favorable conditions. In temperate species, bud dormancy is  
36 divided into three stages depending on the inhibiting factor (Lang *et al.*, 1987). During  
37 paradormancy, other organs such as apical bud or leaves inhibit meristem growth. During  
38 endodormancy, growth is inhibited by factors intrinsic to the bud (‘endo’) whereas during  
39 ecodormancy, growth is limited by environmental factors (‘eco’). During the transition from  
40 growth to dormancy, different phenological stages are visible (*e.g.* growth cessation, leaf fall,  
41 lignification or budset), whereas others are cryptic (*e.g.* endodormancy induction and release).

42 In autumn, endodormancy release is under the control of decreasing temperature and  
43 photoperiod (Welling *et al.*, 2002; Arora *et al.*, 2003; Maurya & Bahlerao, 2017). After  
44 endodormancy is released, cryptic growth of ecodormant buds progresses under the control of  
45 warm temperature, in most species, eventually modulated by photoperiod in photosensitive  
46 species, such as late successional species (Basler & Körner, 2012). Process-based models using  
47 these variables as input have been developed to simulate the endodormancy release and  
48 budbreak dates (Caffarra *et al.*, 2011a; Chuine *et al.*, 2016).

49 In the context of global change, it is particularly critical to accurately predict future trends  
50 in warmer climates. Since the first empirical model describing the relation between temperature  
51 and plant development, through the concept of thermal-time (Réaumur, 1735), budbreak and  
52 flowering models have only computed the accumulation of growth-effective temperature (*i.e.*  
53 growth degree days GDD). As the starting point is set at the coldest time of the year (*i.e.* January  
54 1<sup>st</sup> or July 1<sup>st</sup> in the northern and southern hemispheres, respectively), these models provide  
55 accurate results. However, this type of model is not effective in regions with warmer winters,

56 where attempts have been made to grow temperate crop species (*e.g.* in North Africa, the  
57 Middle East or South America; Balandier *et al.*, 1993). In this context, temperate perennial  
58 crops exhibit a lack of chilling and insufficient endodormancy release (Weinberger, 1950). The  
59 process of endodormancy, and the related chilling accumulation, had therefore been introduced  
60 into the models (Weinberger, 1956; Vegis 1964). Different chilling accumulation functions  
61 have been developed, depending on the species. An important difference is the consideration  
62 of a delaying effect on endodormancy release for warm temperature (*e.g.* Utah model;  
63 Richardson *et al.*, 1974) or not (*e.g.* Chilling hours; Weinberger, 1967). In recent decades,  
64 naturally growing trees have also been affected by a reduction in chilling exposure throughout  
65 winter, increasing interest in the endodormancy stage (Gauzere *et al.*, 2019).

66 Two-step models, simulating endo- and ecodormancy stages, are now commonly used to  
67 predict budbreak dates (Chuine *et al.*, 2016). In perennial plants, the completion of one stage is  
68 concomitant with the onset of the following one (Hänninen & Tanino, 2011). However, the  
69 initial date for chilling accumulation ( $D_{CA}$ ) is usually set arbitrarily with various rules resulting  
70 in huge variability between studies (from late summer until late autumn). Four different  
71 concepts of  $D_{CA}$  were used (see Tab. S1):

- 72 - Fixed date across years and locations: from 1 September (Chuine *et al.*, 2016) to 1  
73 November (Weinberger, 1967) for the northern hemisphere,
- 74 - Flexible date through a simple climatic threshold: critical temperature (*e.g.* date of first frost;  
75 Landsberg, 1974) or photoperiod (Welling *et al.*, 1997),
- 76 - Flexible date through a mathematic function using a single variable such as the date of  
77 minimum chilling units computed by the Utah model (Richardson *et al.*, 1974),
- 78 - Flexible date through a mathematic function using interacting variables (temperature and  
79 photoperiod) simulating leaf fall date (Delpierre *et al.*, 2009) or endodormancy induction  
80 (DORMPHOT; Caffarra *et al.*, 2011a).

81 By aggregating data from 1975 until 2019 in different orchards across France for *J. regia* cv  
82 Franquette, different computations were tested to simulate the effects of the onset of chilling  
83 accumulation  $D_{CA}$  on the predictive accuracy of endodormancy release and budbreak dates.  
84 Specifically, we tested whether the use of dynamic  $D_{CA}$  could account for the delaying effect  
85 of warm temperature on endodormancy release by comparing positive and positive/negative  
86 chilling functions. In a second step, the optimal model was evaluated for the prediction of future  
87 climate over France under three contrasting climatic *scenarii*.

## 88 **Material and methods**

### 89 *Dormancy depth and endodormancy release*

90 Endodormancy release dates were measured using the one-node-cutting ‘forcing’ test of  
91 Rageau (1982). Sampling was performed every three weeks from October to March and 48 one-  
92 node cuttings were prepared per sampling date. Buds were isolated from other parts of plant to  
93 avoid correlative inhibitions (Dennis, 2003). On each sampling date, one-year-old stems were  
94 sampled from five individual trees and cut into 7-cm long pieces, bearing only one node at the  
95 top or less than 1 cm below the upper end, for terminal and axillary buds, respectively. For  
96 axillary buds, the top of the cutting was covered with paraffin to prevent desiccation. The bases  
97 of the cuttings were immersed in tap water, changed weekly. Forty-eight cuttings were exposed  
98 to optimal conditions for growth resumption (*i.e.* 16/8 hours Day/Night and 25°C constant) and  
99 observed individually every 3 days. Mean time until budbreak (stage 09 BBCH; Meier, 2001)  
100 was computed from individual time until budbreak for each cutting. After endodormancy  
101 release, buds of *J. regia* cv Franquette break out after 20 days under optimal conditions  
102 (Mauget, 1980; Charrier *et al.*, 2011). The endodormancy release dates were therefore obtained  
103 by linear interpolation between the two dates giving a time to budbreak greater than (or equal  
104 to) and less than (or equal to) 20 days, respectively.

### 105 *Budbreak dates*

106 Budbreak in the field was monitored every two to three days at the different sites, on five  
107 individual trees until 50% of buds reached the BBCH stage 09. The different sites and number  
108 of annual observations are shown in Table 1.

#### 109 *Climatic data*

110 The models were fit using the daily average and minimal temperatures observed by the weather  
111 stations, mostly located in the same orchard and within 10km distance (Tab. 1). For prediction,  
112 temperatures, calculated according to the CNRM-ALADIN52 model and corrected by a Q-Q  
113 method (Déqué *et al.*, 2007), were used from 8462 sites across France (Safran grid at 64km<sup>2</sup>  
114 spatial resolution; MétéoFrance). Four datasets were used as input variable: the reference period  
115 (1950-2005) and three contrasting climate *scenarii* (RCP 2.6, RCP 4.5 and RCP 8.5) for the  
116 future period: short-term (2006-2051) and long-term (2051-2100). For each site, day length was  
117 computed as a function of latitude and day of year.

#### 118 *Endodormancy induction and onset of chilling accumulation*

119 The initial date for chilling accumulation ( $D_{CA}$ ) was computed using different functions:

- 120 i) Fixed date as a Julian Day.
- 121 ii) Flexible date based on threshold values reached by minimum temperature ( $T_{min}$ ), mean  
122 temperature ( $T_{mean}$ ), first frost (FF) or photoperiod.
- 123 iii) Date of minimum chilling units ( $CU_{min}$ ) computed according to the Utah model (originally  
124 developed on *Prunus persica* L. Batsch) which computes the negative chilling effect for  
125 temperature above 16°C (Richardson *et al.*, 1974). Daily CU were summed from DOY 182  
126 (1 July) until DOY 365 (31 December) using the Utah\_Model function (ChillR package;  
127 Luedeling, 2019) as follows:

$$128 \quad CU[\theta(t)] = \begin{cases} 0 & \text{if } \theta(t) < 1.4 \\ 0.5 & \text{if } 1.5\theta(t) < 2.4 \\ 1 & \text{if } 2.5 < \theta(t) < 9.1 \\ 0.5 & \text{if } 9.2 < \theta(t) < 12.4 \\ 0 & \text{if } 12.5 < \theta(t) < 15.9 \\ -0.5 & \text{if } 16 < \theta(t) < 18 \\ -1 & \text{if } \theta(t) > 18 \end{cases} \quad (1)$$

129 with  $\theta(t)$  the daily mean temperature.

130 iv) Predicted leaf fall dates (BBCH 97) computed according to the thermal (LFT) and  
 131 photothermal (LFPT) models developed by Delpierre *et al.* (2009) for *Quercus* and  
 132 *Quercus + Fagus*, respectively. Below a critical photoperiod  $P_{start}$  and for a temperature  
 133 colder than a threshold  $T_b$ , the variable  $R_{sen}$ , modulated by a photoperiod function in the  
 134 case of the LFPT model, is summed up to a critical value ( $Y_{crit}$ ), corresponding to the leaf  
 135 fall date. Both LFT and LFPT models were computed using the original or optimized  
 136 parameter sets: LF(P)T<sub>ori</sub> and LF(P)T<sub>adj</sub>, respectively.

$$137 \quad R_{sen}[\theta(t); P(t)] = \begin{cases} 0 & \text{if } P(t) \geq P_{start} \\ 0 & \text{if } \theta(t) \geq T_b \\ [\theta(t) - T_b]^2 \times \left(1 - \frac{P(t)}{P_{start}}\right)^y & \text{if } \theta(t) < T_b \end{cases} \quad (2)$$

138 with  $\theta(t)$  the daily mean temperature and  $P(t)$  the photoperiod. The parameter  $y$  was set to 0 and  
 139 2 for LFT and LFPT models, respectively.

140 v) The endodormancy induction state (DS) was computed according to the DORMPHOT  
 141 model developed for *Betula pubescens* Ehrh. by Caffarra *et al.* (2011a). The two sigmoidal  
 142 response functions to low temperature and photoperiod interact to compute DS. When  $\Sigma DS$   
 143 reaches  $D_{crit}$ , the date is reported as  $D_{CA}$ . Both the original (DP<sub>ori</sub>) and optimized (DP<sub>adj</sub>)  
 144 parameter sets were used.

$$145 \quad DS[\theta(t); P(t)] = \frac{1}{1+e^{aD(\theta(t)-bD)}} \times \frac{1}{1+e^{10(24-P(t)-DL_{crit})}} \quad (3)$$

146 with  $\theta(t)$  the daily mean temperature,  $P(t)$  the photoperiod,  $aD$  a coefficient for the effect of  
 147 temperature,  $bD$  a critical temperature and  $DL_{crit}$  a critical photoperiod.

149 From  $D_{CA}$ , the effect of chilling temperature was simulated according to the inverse of the  
 150 Richardson function (Richardson *et al.*, 1974). This function was defined as the best function  
 151 predicting endodormancy release dates in walnut trees, although it does take into account the  
 152 negation of chilling at warm temperature (Chuine *et al.*, 2016; Charrier *et al.*, 2018). According  
 153 to the sequential paradigm, the date at which  $CU(t)$  reaches the critical  $CU_{crit}$  threshold  
 154 (arbitrary chilling units,  $CU$ ) is the date of endodormancy release ( $D_{ER}$ ), or the transition from  
 155 endodormancy to ecodormancy:

$$156 \quad CU(t + 1) = CU(t) + Max[Min(T_{high} - \theta(t); T_{high} - T_{low}); 0] \quad (4)$$

157 with  $CU(t)$  the chilling unit on day  $t$ ,  $T_{high}$  the temperature above which  $CU(t)$  is 0 and  $T_{low}$  the  
 158 temperature below which  $CU(t)$  is maximum;  $CU(t)$  is linear between  $T_{low}$  and  $T_{high}$ .

159 Alternatively, the smoothed-Utah function, a smoothed version of the Utah function proposed  
 160 by Richardson *et al.* (1974), takes into account the negation of chilling on warm days  
 161 (Bonhomme *et al.*, 2010).

$$162 \quad CU(t + 1) = CU(t) + \begin{cases} \frac{1}{1 + e^{-4\frac{\theta(t) - T_{m1}}{T_{opt} - T_{m1}}}} \text{ if } \theta(t) > T_{m1} \\ \frac{0.5(\theta(t) - T_{opt})^2}{(T_{m1} - T_{opt})^2} \text{ if } T_{m1} < \theta(t) < T_{opt} \\ 1 - (1 - \min) \frac{0.5(\theta(t) - T_{opt})^2}{(T_{m1} - T_{opt})^2} \text{ if } T_{opt} < \theta(t) < T_{n2} \\ \min + \frac{1 - \min}{1 + e^{-4\frac{T_{n2} - \theta(t)}{T_{n2} - T_{opt}}}} \text{ if } T_{n2} < \theta(t) \end{cases} \quad (5)$$

163 with  $CU(t)$  the chilling unit at day  $t$ ,  $T_{opt}$  the optimal temperature for chilling,  $T_{m1}$  the slope of  
 164 the cold efficiency at a colder temperature than  $T_{opt}$ ,  $T_{n2}$  the temperature warmer than  $T_{opt}$   
 165 which has half the efficiency of  $T_{opt}$  to release endodormancy;  $\min$  the effect of warm  
 166 temperature to delete previously accumulated  $CU$ .

167 The ontogenetic development during ecodormancy stage was modeled according to a  
168 sigmoid function (Caffarra *et al.*, 2011a). The date when  $FU(t)$  reaches the critical threshold  
169  $FU_{crit}$  (arbitrary forcing units,  $FU$ ) is the budburst date ( $D_{BB}$ ).

$$170 \quad FU(t + 1) = FU(t) + \frac{1}{1 + e^{-slp(\theta(t) - T_{50})}} \quad (6)$$

171 with  $FU(t)$  the forcing unit at day  $t$ ,  $slp$  the slope of the function at the temperature inducing  
172 half of the maximal apparent growth rate  $T_{50}$ .

### 173 *Model calibration depending on the onset of chilling accumulation*

174 For a given  $D_{CA}$  rule, endodormancy release date was calibrated first and the best set of  
175 parameters was used to calibrate the bud break date. The nls function (using Gauss-Newton  
176 algorithm, R ver.3.6.2; R development Core Team, 2019) was used to minimize the sums of  
177 square between the observed and predicted values with different sets of starting values at the  
178 minimum, average and maximum ranges of realistic parameter values. In order to maximize the  
179 variability within the datasets, half of the observation per site was assigned to the calibration  
180 dataset, the other half to the validation dataset. Two independent calibration procedure were  
181 performed using symmetrical datasets. For an odd number of observations per site, one more  
182 observation per site was included in the calibration set #1.

183 For the endodormancy release model, in addition to the parameters defining  $D_{CA}$ , three  
184 parameters were optimized:  $T_{low}$  and  $T_{high}$  corresponding to the temperature thresholds and  
185  $CU_{crit}$  the sum of chilling units to release endodormancy.

186 For the ecodormancy model, one parameter was optimized:  $FU_{crit}$  corresponding to the sum  
187 of forcing units for bud break. The endodormancy model used to predict  $D_{ER}$  was the best from  
188 the previous step and the other parameters ( $slp$  and  $T_{50}$ ) set to the values described in Charrier  
189 *et al.* (2018).

190 The quality of the fit and predictive ability of the models in relation to the  $D_{CA}$  were assessed  
191 for calibration and validation datasets by computing Root Mean Square Error (RMSE),  
192 Predictive Root Mean Square Error (RMSEP) and Akaike Index Criterion ( $AIC_C$ ):

$$193 \quad RMSE(P) = \sqrt{\frac{\sum_{i=1}^n (\hat{y}_i - y_i)^2}{n}} \quad (7)$$

194 with  $\hat{y}_i$  the predicted values for an observation  $i$  and  $y_i$  the observed values for an observation  $i$

$$195 \quad AIC_C = 2n \left[ \log(RMSE) + \frac{k}{n-k-1} \right] \quad (8)$$

196 with  $k$  the number of parameters,  $n$  the number of observations.

### 197 *Correlations between simulated and climate variables*

198 Correlations between the mean endodormancy onset date, mean endodormancy release date  
199 ( $D_{ER}$ ) and mean budbreak date ( $D_{BB}$ ) per site (8462 sites at 64km<sup>2</sup> spatial resolution) and mean  
200 annual temperature were fitted by minimizing the sums of squares using a non-linear regression  
201 procedure (function `nls` in R). Different functions were tested: linear, sigmoid, exponential,  
202 power, second, third or fourth degree polynomial) and selected according to RMSE and  $AIC_C$ .

## 203 **Results**

### 204 *Dormancy stages*

205 During the endodormancy induction stage, the time to bud break generally increased by 20 days  
206 between August and October and reaches a maximum value (50-80 days) between October and  
207 December (Figure 1). The endodormancy release is observed when the time to bud break  
208 gradually decreased to 20 days. The transition from endodormancy to ecodormancy is marked  
209 by a breaking point in the curves between mid-December and mid-February. Significant  
210 correlations were observed between the onset of endodormancy and the date of maximum depth  
211 of dormancy ( $P = 0.005$ ; Fig. 1B) and between the date of maximum depth of dormancy and

212 the date of endodormancy release ( $D_{ER}$ ;  $P = 0.030$ ; Fig. 1C). However, no correlation was  
213 observed between the onset of endodormancy and  $D_{ER}$  ( $P = 0.387$ ; Fig. 1D).

#### 214 *Effects of $D_{CA}$ on endodormancy release date*

215 The use of different rules to compute the initial date for chilling accumulation ( $D_{CA}$ ) had a  
216 relatively small effect on the prediction of  $D_{ER}$  (Tab. 2). The use of a positive chilling function  
217 was overall more efficient than functions that take into account the delaying effect of warm  
218 temperature (positive and negative). For most rules, 75% of the RMSEs were within 2-3 days:  
219 between 11.5 and 13.3 days and between 7.2 and 9.5 days for dataset #1 and #2, respectively.  
220 However, the uses of FF and  $CU_{min}$  ori were not effective for both datasets. The predictive  
221 ability was relatively good for most of the  $D_{CA}$ , with 75% RMSEP between 8.3 and 11.6 days  
222 and between 12.9 and 14.4 days for dataset #1 and #2, respectively. Finally, considering the  
223 rule that provided values below 125% of the minimum for RMSE and RMSEP in both datasets,  
224 only a few rules appeared satisfactory: Photoperiod and LFPT adj (positive only),  $CU_{min}$  adj  
225 (positive & negative), LFPT ori, DORMPHOT ori and DORMPHOT adj (positive only and  
226 positive & negative). By increasing the stringency to 110%, only DORMPHOT adj (positive  
227 only) could be considered an accurate and robust model.

#### 228 *Effects of $D_{CA}$ on budburst date*

229 The accuracy of the fits was slightly better for budbreak date ( $D_{BB}$ ) than for  $D_{ER}$  (Tab. 3),  
230 although the effect of the different rules on  $D_{BB}$  was relatively similar to that observed for  $D_{ER}$ .  
231 The use of the positive chilling function was more effective than positive & negative functions.  
232 For most of the  $D_{CA}$ , 75% of the RMSEs were within a 2-3 days range: between 7.4 and 9.6  
233 days and between 6.8 and 8.6 days for dataset #1 and #2, respectively. The uses of FF and  $CU_{min}$   
234 ori were also less efficient. The predictive ability was less than one week for most  $D_{CA}$ , with  
235 75% of RMSEP between 6.7 and 9.3 days and between 6.9 and 8.2 days for dataset #1 and #2,  
236 respectively. Considering the  $D_{CA}$  that had values below 125% of the minimum for RMSE and

237 RMSEP for both datasets, most of the rules, with the exception of FF and  $CU_{\min}$  ori, appeared  
238 satisfactory. By increasing the stringency to 110%, several rules remained accurate and robust:  
239 Julian day and photoperiod, LFPT adj (positive only), LFT ori (positive & negative), LFPT ori  
240 and DORMPHOT ori (positive only and positive & negative). Finally, with the exception of FF  
241 and  $CU_{\min}$  ori, all models provided relatively accurate phenological predictions for  $D_{ER}$   
242 (RMSEP <15 days) and  $D_{BB}$  (RMSEP < 8 days), but DORMPHOT adj (positive only) can be  
243 considered the best.

#### 244 *Predictions under current and future climates for Juglans regia cv Franquette*

245 DORMPHOT adj (positive only) was used to explore the current and future phenology trend.  
246  $D_{CA}$ ,  $D_{ER}$  and  $D_{BB}$  have a structured geographical distribution across France (Fig. 2).  $D_{CA}$   
247 spanned a range of 43 days: earlier in the mountain areas (Mid-August) and later on the  
248 Mediterranean (South East; Late September) and south-western coasts (Late August – Mid-  
249 September).  $D_{ER}$  had a similar distribution but over a wider range (84 days): from the beginning  
250 of December in mountain areas to the end of February on the Mediterranean coast.  $D_{BB}$  showed  
251 an opposite distribution over a period of 72 days: from mid-April in the southern and western  
252 regions to the end of June in the mountainous areas.

253  $D_{CA}$ ,  $D_{ER}$  and  $D_{BB}$  were strongly correlated with the mean annual temperature (MAT),  
254 although following different functions (exponential for  $D_{CA}$  and  $D_{ER}$  and cubic function for  
255  $D_{BB}$ ; Fig. 3). Similar trends were observed in future climate predictions, with close relationships  
256 between MAT and  $D_{CA}$ ,  $D_{ER}$  or  $D_{BB}$  (Fig. 4). The functions describing the relationships between  
257 MAT and  $D_{CA}$  and  $D_{ER}$  were monotonic. Warmer temperatures, as predicted by the different  
258 climate scenario, are therefore expected to delay the onset of chilling accumulation by 5-6 days  
259 until 2050 and, by the end of the century, by up to 20 days according to the RCP 8.5 *scenario*  
260 (Fig. 4A; G). Consequently, endodormancy release would be delayed by 6-7 days until 2050  
261 and, by the end of the century, by up to 24 days under the RCP 8.5 *scenario* (Fig. 4B; H).

262 However, the delay in the release of endodormancy did not directly affect the  $D_{BB}$ . The  
263 relationship between  $D_{BB}$  and temperature shows a tipping point *i.e.* a temperature higher than  
264 13.83°C would induce later  $D_{BB}$  (Fig. 3C).  $D_{BB}$  would occur only 3-4 days earlier until 2050  
265 (Fig. 4C; I). By the end of the century, bud break is expected to be earlier under RCP 4.5  
266 *scenario* (-6.4 days) than under the warmer RCP 8.5 *scenario* (-3.5 days). Finally, a later bud  
267 break than today is likely to occur in an increasing portion of the France at the end of the 21<sup>st</sup>  
268 century: from 5.6 (RCP 4.5) to 33.8% (RCP8.5) of the French territory in 2051-2100 (Fig. 5).  
269 Considering the main French production areas, *i.e.* ‘Noix de Grenoble’ (Middle East) and ‘Noix  
270 du Périgord’ (Middle West) Protected Designation of Origin (PDO) areas, bud break would be  
271 delayed in most of the ‘Noix du Périgord’ area (96.8% in RCP 8.5 2051-2100) but not in the  
272 ‘Noix de Grenoble’ area.

273 The current annual variability in phenological stages is similar for  $D_{CA}$  and  $D_{ER}$  (variance of  
274 about 5 days; Fig 4D, E). The future climate would increase the variance in  $D_{CA}$  and  $D_{ER}$   
275 considerably, especially for RCP 8.5 in the 2051-2100 period (about 10 days). However, the  
276 pattern is reversed for  $D_{BB}$ , with variance of 10 days in the current period, while 5-7 days are  
277 expected in the future climate (Fig 4F). In both PDO areas, the variance in  $D_{BB}$  would decrease  
278 by 2-3 days (RCP 8.5 scenario).

## 279 **Discussion**

280 The definition of the initial date for simulating cyclic processes is a key issue. To predict the  
281 annual phenological cycle in perennial organisms, such as trees, various empirical rules have  
282 been used so far. The onset of chilling accumulation during the endodormancy stage ( $D_{CA}$ ) had,  
283 for instance, been arbitrarily set using fixed dates regardless of year and location (Chuine *et al.*,  
284 2016) or depending of environmental factors controlling the induction of endodormancy  
285 (Caffarra *et al.*, 2011b). In the current study, long-term observations of phenological stages  
286 (endodormancy release  $D_{ER}$  and bud break  $D_{BB}$ ) were used to define the most efficient rule

287 under various environmental conditions. For most computations, the different rules for defining  
288  $D_{CA}$  did not have a large impact on the accuracy of endodormancy release and bud break dates  
289 (*ca.* 2-3 days; Tab. 2-3). Overall, using a function that computes the negative effect of warm  
290 temperature, such as the Utah model, did not improve accuracy. Using a relevant  $D_{CA}$  is  
291 therefore more robust than negating early chilling accumulation in walnut in France as was also  
292 observed using a fixed  $D_{CA}$  date (Chuine *et al.*, 2016).

293 Across years and sites, the large ranges of variation for the date of endodormancy induction,  
294 date of maximum dormancy and date of endodormancy release (more than 2 month) suggest  
295 that they cannot be predicted by a simple trigger such as a fixed date or photoperiod (Caffarra  
296 *et al.*, 2011a). Furthermore, the strong correlation between the onset of endodormancy induction  
297 (August - October) and the maximum depth of dormancy (October – December) indicates that  
298 the duration of endodormancy is generally 2 month with a relatively small effect of  
299 environmental conditions (Fig. 1). In contrast, the maximum depth of endodormancy and  
300 endodormancy release are less correlated although significant, temperature being the main  
301 driver of endodormancy release (Weinberger, 1959). However, it is not clear whether chilling  
302 temperature actually acts only during endodormancy release or already during the induction of  
303 endodormancy.

304 The optimization of the different models showed that the different rules for defining the  $D_{CA}$   
305 do not induce large variations in the predicting of  $D_{ER}$  and  $D_{BB}$  from September to November.  
306 However, the date of the first frost event and the date of  $CU_{min}$  were less efficient than the other  
307 rules. All relevant rules for dataset #2 considered a potential effect of photoperiod, either  
308 directly or indirectly via the fixed date (Welling *et al.*, 1997; Chuine and Régnière, 2017). The  
309 DORMPHOT model, originally developed in *Betula pubescens*, is relevant for other deciduous  
310 species such as *Juglans regia*. The optimal date for chilling accumulation is in late summer  
311 (mean date 28 August), suggesting that buds actually integrate information from chilling

312 exposure during budset although MTB is only beginning to increase. The use of a critical  
313 photoperiod (*e.g.* 12h observed on September 21<sup>st</sup>) or a fixed date (*e.g.* 1 September; Chuine et  
314 al., 2016) is therefore relatively relevant, although it may be shifted by 20 days in the future  
315 climate (Fig. 4).

316 The conceptual development of the DORMPHOT model is based on experimental results  
317 combining the manipulation of photoperiod and temperature (Caffarra *et al.*, 2011b), whereas  
318 other formalisms were based on empirical observations (*e.g.* leaf fall; Delpierre *et al.*, 2009).  
319 Temperature and photoperiod are closely correlated over the seasons. However, temperature  
320 fluctuations are much larger at a given time of the year, which could induce greater variability  
321 in the onset of endodormancy if it were the only controlling factor (Fig.1). As the induction of  
322 endodormancy is a lengthy process (*ca.* 2 month), perennial plants cannot rely solely on  
323 temperature changes that may be too sudden to induce winter dormancy in time (Caffarra *et al.*,  
324 2011a). Photoperiod and temperature variables therefore affect the annual phenological cycle  
325 of perennial plants, although to different extents in different species. For example, photoperiod  
326 is dominant in *Populus* (Kalcsits *et al.*, 2009) and *Vitis* (Fennel & Hoover, 1991), while  
327 temperature is dominant in *Malus*, *Pyrus* (Heide & Prestrud, 2005) and *Sorbus* (Heide, 2011).  
328 The interaction between photoperiod and temperature has been demonstrated in *Prunus* (Heide,  
329 2008). It has been hypothesized that the modulation of photoperiod sensitivity by temperature  
330 might be related to the thermal effect on day length perception by phytochromes (Mølmann *et*  
331 *al.*, 2005).

332 The rule selected for the  $D_{CA}$  predicted a delayed onset of chilling accumulation in warmer  
333 locations in France ( $> 7^{\circ}\text{C}$  MAT; Fig. 3A). Warmer temperature indeed delays the induction of  
334 endodormancy in different species (Beil *et al.*, 2021). Such a delay would further delay the  
335 release of endodormancy (Fig. 3 B; Caffarra *et al.*, 2014; Chuine *et al.*, 2016). However, after  
336 endodormancy release, cold temperature would limit ontogenetic development during

337 ecodormancy, providing a negative spatial picture of  $D_{BB}$  compared to  $D_{ER}$  (Fig. 2B-C). Under  
338 current climatic conditions, chilling requirements are generally fulfilled annually and therefore  
339 play a minor role in  $D_{BB}$  variations (Gauzere *et al.*, 2017). Using a sensitivity analysis with a  
340 fixed  $D_{CA}$ , Gauzere *et al.* (2019) also observed a minor role of  $D_{CA}$  in predicting  $D_{BB}$  only.  
341 Comparison of the two phenological stages showed that the role of  $D_{CA}$  was more important in  
342 predicting  $D_{ER}$  than  $D_{BB}$  (Tab.2-3). As many studies are based on  $D_B$ , only, without information  
343 on  $D_{ER}$ , many different formalisms seem valid and are commonly used for phenological  
344 modeling (Tab. S1). However, the use of experimental results to fit phenological models is  
345 essential to ensure that the fitted functions remain realistic (Chuine *et al.*, 2016; Hänninen *et*  
346 *al.*, 2019). Finally, the  $D_{CA}$  simulated by the DORMPHOT model provided the most accurate  
347 predictions for  $D_{ER}$  and  $D_{BB}$  in both datasets.

348 Under future climate conditions as predicted by the RCP *scenarii*, the tipping point for  $D_{BB}$   
349 ( $MAT = 13.86^{\circ}C$ ) would be reached in a larger fraction of France. Above the  $13.86^{\circ}C$  threshold,  
350 induction and release of endodormancy would be more delayed than ecodormancy hastened,  
351 resulting in delayed bud break compared to the current period. Delayed bud break would thus  
352 cover up to one quarter of France under RCP 8.5 *scenario* in 2051-2100 (Fig. 5). Such a lack  
353 of chilling during endodormancy has also been assumed for apricot in the UK (Martínez-  
354 Lüscher *et al.*, 2017). Interestingly, in the future climate, the annual variability in  $D_{BB}$  is  
355 expected to be lower. The trend towards a more uniform  $D_{BB}$  has already been observed in  
356 recent decades (Vitasse *et al.*, 2018). A more uniform phenology would act as a stabilizing  
357 factor for fruit production by synchronizing pollination and ripening. However, the lack of  
358 chilling temperature during endodormancy induces severe agronomic issues such as erratic  
359 patterns of blooming, floribondity, and potential dischronism with anthesis (Campoy *et al.*,  
360 2011). An accurate assessment of temperature response during endodormancy is therefore  
361 necessary to complement the experimental data obtained during the ecodormancy stage

362 (Charrier *et al.*, 2011). It would clarify the future of the French walnut production area. The  
363 two PDO areas would indeed face distinct threats as they are on opposite sides of the tipping  
364 point. In the Périgord, chilling requirements are likely not to be fulfilled and varieties with  
365 lower chilling requirements need to be developed, as current varieties do not exhibit variability  
366 for this trait (Charrier *et al.*, 2011). In Grenoble, earlier budbreak dates are expected, leading to  
367 greater exposure to late frost events, and varieties with higher forcing requirements can help  
368 stabilize production (Charrier *et al.*, 2018).

### 369 **Conclusions and perspectives**

370 This study highlighted the relevance of using flexible dates to initiate chilling accumulation  
371 rather than functions that compute the negative chilling accumulation at warm temperature. The  
372 DORMPHOT model, integrating the control of endodormancy induction by temperature and  
373 photoperiod, is the most efficient in predicting endodormancy and ecodormancy stages. The  
374 tipping point of phenological processes will probably be reached during the 21<sup>st</sup> century with  
375 chilling requirements that are likely to be fulfilled later or not at all. Although these results are  
376 important for walnut production, the observed correlation between MAT and phenological  
377 stages represents a relevant tool for building meta-models valid in many species at the global  
378 scale.

## REFERENCES

- Arora, R., Rowland, L. J., & Tanino, K. (2003). Induction and release of bud dormancy in woody perennials: a science comes of age. *HortScience*, 38(5), 911-921.
- Balandier, P., Gendraud, M., Rageau, R., Bonhomme, M., Richard, J. P., & Parisot, E. (1993). Bud break delay on single node cuttings and bud capacity for nucleotide accumulation as parameters for endo-and paradormancy in peach trees in a tropical climate. *Scientia Horticulturae*, 55(3-4), 249-261.
- Basler, D., & Körner, C. (2012). Photoperiod sensitivity of bud burst in 14 temperate forest tree species. *Agricultural and Forest Meteorology*, 165, 73-81.
- Beil, I., Kreyling, J., Meyer, C., Lemcke, N., & Malyshev, A. V. (2021). Late to bed, late to rise—Warmer autumn temperatures delay spring phenology by delaying dormancy. *Global Change Biology*.
- Caffarra, A., Donnelly, A., Chuine, I., & Jones, M. B. (2011a). Modelling the timing of *Betula pubescens* budburst. I. Temperature and photoperiod: a conceptual model. *Climate Research*, 46(2), 147-157.
- Caffarra, A., Donnelly, A., & Chuine, I. (2011b). Modelling the timing of *Betula pubescens* budburst. II. Integrating complex effects of photoperiod into process-based models. *Climate research*, 46(2), 159-170.
- Caffarra, A., Zottele, F., Gleeson, E., & Donnelly, A. (2014). Spatial heterogeneity in the timing of birch budburst in response to future climate warming in Ireland. *International journal of biometeorology*, 58(4), 509-519.
- Campoy, J. A., Ruiz, D., & Egea, J. (2011). Dormancy in temperate fruit trees in a global warming context: a review. *Scientia Horticulturae*, 130(2), 357-372.
- Charrier, G., Bonhomme, M., Lacoïnte, A., & Améglio, T. (2011). Are budburst dates, dormancy and cold acclimation in walnut trees (*Juglans regia* L.) under mainly genotypic or environmental control?. *International journal of biometeorology*, 55(6), 763-774.
- Charrier, G., Chuine, I., Bonhomme, M., & Améglio, T. (2018). Assessing frost damages using dynamic models in walnut trees: exposure rather than vulnerability controls frost risks. *Plant, Cell & Environment*, 41(5), 1008-1021.
- Chuine, I., & Régnière, J. (2017). Process-based models of phenology for plants and animals. *Annual Review of Ecology, Evolution, and Systematics*, 48, 159-182.
- Chuine, I., Bonhomme, M., Legave, J. M., García de Cortázar-Atauri, I., Charrier, G., Lacoïnte, A., & Améglio, T. (2016). Can phenological models predict tree phenology accurately in the future? The unrevealed hurdle of endodormancy break. *Global Change Biology*, 22(10), 3444-3460.
- Delpierre, N., Dufrêne, E., Soudani, K., Ulrich, E., Cecchini, S., Boé, J., & François, C. (2009). Modelling interannual and spatial variability of leaf senescence for three deciduous tree species in France. *Agricultural and Forest Meteorology*, 149(6-7), 938-948.
- Dennis, F. G. (2003). Problems in standardizing methods for evaluating the chilling requirements for the breaking of dormancy in buds of woody plants. *HortScience*, 38(3), 347-350.
- Déqué, M., Rowell, D. P., Lüthi, D., Giorgi, F., Christensen, J. H., Rockel, B., ... & van den Hurk, B. J. J. M. (2007). An intercomparison of regional climate simulations for Europe: assessing uncertainties in model projections. *Climatic Change*, 81(1), 53-70.
- Gauzere, J., Delzon, S., Davi, H., Bonhomme, M., de Cortazar-Atauri, I. G., & Chuine, I. (2017). Integrating interactive effects of chilling and photoperiod in phenological process-based models. A case study with two European tree species: *Fagus sylvatica* and *Quercus petraea*. *Agricultural and Forest Meteorology*, 244, 9-20.

- Gauzere, J., Lucas, C., Ronce, O., Davi, H., & Chuine, I. (2019). Sensitivity analysis of tree phenology models reveals increasing sensitivity of their predictions to winter chilling temperature and photoperiod with warming climate. *Ecological Modelling*, *411*, 108805.
- Hänninen, H., Kramer, K., Tanino, K., Zhang, R., Wu, J., & Fu, Y. H. (2019). Experiments are necessary in process-based tree phenology modelling. *Trends in Plant Science*, *24*(3), 199-209.
- Hänninen, H., & Tanino, K. (2011). Tree seasonality in a warming climate. *Trends in plant science*, *16*(8), 412-416.
- Heide, O. M. (2008). Interaction of photoperiod and temperature in the control of growth and dormancy of *Prunus* species. *Scientia Horticulturae*, *115*(3), 309-314.
- Heide, O. M. (2011). Temperature rather than photoperiod controls growth cessation and dormancy in *Sorbus* species. *Journal of experimental botany*, *62*(15), 5397-5404.
- Heide, O. M., & Prestrud, A. K. (2005). Low temperature, but not photoperiod, controls growth cessation and dormancy induction and release in apple and pear. *Tree physiology*, *25*(1), 109-114.
- Kalcsits, L. A., Silim, S., & Tanino, K. (2009). Warm temperature accelerates short photoperiod-induced growth cessation and dormancy induction in hybrid poplar (*Populus* × spp.). *Trees*, *23*(5), 971-979.
- Landsberg, J. J. (1974). Apple fruit bud development and growth; analysis and an empirical model. *Annals of Botany*, *38*(5), 1013-1023.
- Lang, G. A., Early, J. D., Martin, G. C., & Darnell, R. L. (1987). Endo-, para-, and ecodormancy: physiological terminology and classification for dormancy research. *HortScience*, *22*(3), 371-377.
- Luedeling, E. (2019) Statistical Methods for Phenology Analysis in Temperate Fruit Trees, chillR Package.
- Martínez-Lüscher, J., Hadley, P., Ordidge, M., Xu, X., & Luedeling, E. (2017). Delayed chilling appears to counteract flowering advances of apricot in southern UK. *Agricultural and Forest Meteorology*, *237*, 209-218.
- Mauget, J. C., (1980). Dormance et précocité de débourrement des bourgeons chez quelques cultivars de Noyer (*Juglans regia* L.).
- Maurya, J. P., & Bhalerao, R. P. (2017). Photoperiod-and temperature-mediated control of growth cessation and dormancy in trees: a molecular perspective. *Annals of botany*, *120*(3), 351-360.
- Meier, U. (2001). Growth stages of mono- and dicotyledonous plants. BBCH Monograph. doi: 10.5073/bbch0515.
- Møllmann, J. A., Asante, D. K., Jensen, J. B., Krane, M. N., Ernstsén, A., Juntila, O., & Olsen, J. E. (2005). Low night temperature and inhibition of gibberellin biosynthesis override phytochrome action and induce bud set and cold acclimation, but not dormancy in PHYA overexpressors and wild-type of hybrid aspen. *Plant, Cell & Environment*, *28*(12), 1579-1588.
- R Development Core Team (2019) R: A Language and Environment for Statistical computing. <https://www.r-project.org/>
- Rageau, R. (1982). Étude expérimentale des lois d'action de la température sur la croissance des bourgeons floraux du pêcher (*Prunus persica* L. Batsch) pendant la postdormance.
- Réaumur, R. A. F. d. 1735. Observations du thermomètre, faites à Paris durant l'année 1735, comparées avec celles qui ont été faites sous la ligne, à l'isle de France, à Alger et quelques unes de nos isles de l'Amérique. Mémoires de l'Académie des Sciences de Paris.
- Richardson, E. A., EA, R., SD, S., & DR, W. (1974). A model for estimating the completion of rest for "Redhaven" and "Elberta" peach trees.
- Vegis, A. (1964). Dormancy in higher plants. *Annual review of plant physiology*, *15*(1), 185-224.

- Vitasse, Y., Signarbieux, C., & Fu, Y. H. (2018). Global warming leads to more uniform spring phenology across elevations. *Proceedings of the National Academy of Sciences*, 115(5), 1004-1008.
- Weinberger, J. H. (1950). Chilling requirements of peach varieties. In *Proceedings. American Society for Horticultural Science* (Vol. 56, pp. 122-8).
- Weinberger, J. H. (1956). Prolonged dormancy trouble in peaches in the southeast in relation to winter temperatures. *Journal of the American Society for Horticultural Science*, 67, 107-112.
- Weinberger, J. H. (1967). Some temperature relations in natural breaking of the rest of Peach flower buds in the San Joaquin Valley, California. *Proceedings of the American Society for Horticultural Science*, 51, 84-89.
- Welling, A., Kaikuranta, P., & Rinne, P. (1997). Photoperiodic induction of dormancy and freezing tolerance in *Betula pubescens*. Involvement of ABA and dehydrins. *Physiologia Plantarum*, 100(1), 119-125.
- Welling, A., Moritz, T., Palva, E. T., & Junttila, O. (2002). Independent activation of cold acclimation by low temperature and short photoperiod in hybrid aspen. *Plant Physiology*, 129(4), 1633-1641.

## **Acknowledgements**

The author wants to acknowledge the essential contribution of Marc Bonhomme, Aline Faure, Jean-Claude Mauget, Remi Rageau, Jean-Pierre Richard for dormancy release date measurements. Phenological data and stem materials were provided by Neus Aleita, Romain Baffoin, Fabrice Lheureux, Marianne Naudin and Eloise Tranchand. The author is also thankful to Thierry Améglio, André Lacointe and Heikki Hänninen for constructive comments on preliminary versions of the manuscript. Part of the collected data were supported by the Pôle National de Données de la Biodiversité (a.k.a SOERE Tempo) and by a ‘Pari Scientifique’ grant from the division Agroecosystem of INRAE.

## Figure captions

**Table 1** Site and dataset descriptions.

**Table 2.** Quality of the prediction of endodormancy release dates (ER) using different functions and two different calibration datasets. RMSE, RMSEP and AIC lower than 110% of the minimum RMSE or RMSEP are indicated in bold. Dates for onset of chilling accumulation ( $D_{CA}$ ) were either fixed (Julian Day) or computed according to: date of first frost (FF), minimum temperature ( $T_{min}$ ), mean temperature ( $T_{mean}$ ), photoperiod, minimum chilling unit ( $CU_{min}$ ), leaf fall using temperature (LFT) or temperature and photoperiod (LFPT) and dormancy induction state using the DORMPHOT model (DP). Ori and adj refer to the original published version (ori) or adjusted to the data (adj). Chilling effect were only positive, using the reverse Richardson function, or positive at low temperature and negative at warm temperature, using the smoothed Utah function.

**Table 3.** Quality of the prediction of budburst dates (BB) using different functions and two different calibration datasets. RMSE, RMSEP and AIC lower than 110% of the minimum RMSE or RMSEP are indicated in bold. Dates for onset of chilling accumulation ( $D_{CA}$ ) were either fixed (Julian Day) or computed according to date of first frost (FF), minimum temperature ( $T_{min}$ ), mean temperature ( $T_{mean}$ ), photoperiod, minimum chilling unit ( $CU_{min}$ ), Leaf fall using temperature (LFT) or temperature and photoperiod (LFPT) and DORMPHOT (DP). Ori and Adj refer to the original published version (ori) or adjusted to the data (adj). Chilling effect were only positive or positive at low temperature and negative at warm temperature, using the reverse Richardson and smoothed Utah functions respectively.

**Figure 1. A.** Time to break buds under forcing conditions for one node cuttings of *Juglans regia* cv Franquette. Different colors represent the different phenological stages based on the dynamics in time to break buds. **B-D.** Correlations between the onset of endodormancy induction, the maximum endodormancy depth and endodormancy release.

**Figure 2.** Average dates of onset of chilling accumulation (A), endodormancy release (B) and budburst (C) predicted across France under current climatic conditions.

**Figure 3. A-C.** Average date of onset of chilling accumulation (A), endodormancy release (B) and budburst (C) depending on mean annual temperature across France under different climatic *scenarii*. Exponential (A, B) and cubic (C) functions were represented in black dashed lines.

**Figure 4 A-C** Distribution of the mean (A-C) and variance (D-E) in the date of onset of chilling accumulation (A, D), endodormancy release (B, E) and budburst (C, F) in the current period (Ref) or RCP scenario in the early (2006-2050) and late part of the XXI century (2051-2100) in France. **G-I** Distribution of the variation compared to the reference period in the mean date of onset of chilling accumulation (G), endodormancy release (H) and budburst (I). The box represents the upper and lower quartile with the median indicated by a thick black line, the whiskers represents the 1<sup>st</sup> and 9<sup>th</sup> decile, outliers were not represented. Different letters indicate a significantly different distribution across scenario according to the non-parametric Kruskal Wallis test.

**Figure 5.** Relative change compared to the present period in average budburst dates across France according to different climatic *scenarii* (RCP2.6, RCP4.5 and RCP 8.5)

and time periods (2006-2050 and 2051-2100). Earlier and later budburst dates than the current climate are represented in blue and red, respectively.

## Supplementary material

**Table S1.** Formalisms used to define the onset of chilling accumulation (DCA) across various studies aiming at modeling phenology in various species and location: fixed or flexible date. Chilling models are sigmoid (Hanninen, 1990), normal (Chuine, 2000; Chuine et al., 2003), Utah (Richardson et al., 1974) and variations (smoothed Utah: Bonhomme et al., 2010, Positive Utah and positive Chill Unit for low chilling varieties: Gilreath and Buchanan, 1981), Dynamic (Fishman et al., 1987a,b), Chilling Hours (Weinberger; 1967), Bidabé (Bidabé, 1965a, b), Growing Degree Day (Ritchie and NeSmith, 1991). NH and SH mean northern and southern hemisphere, respectively.

**Figure S1.** Average dates of onset of chilling accumulation predicted across France under future climatic *scenarii* (**A, D** RCP 2.6; **B, E** RCP 4.5 and **C, F** RP 8.5). The higher and lower maps represent the short term (**A-C** 2006-2050) and the long term period (**D-F** 2050-2100), respectively.

**Figure S2.** Average dates of endodormancy release predicted across France under future climatic *scenarii* (**A, D** RCP 2.6; **B, E** RCP 4.5 and **C, F** RP 8.5). The higher and lower maps represent the short term (**A-C** 2006-2050) and the long term period (**D-F** 2050-2100), respectively.

**Figure S3.** Average dates of budburst predicted across France under future climatic *scenarii* (**A, D** RCP 2.6; **B, E** RCP 4.5 and **C, F** RP 8.5). The higher and lower maps represent the short term (**A-C** 2006-2050) and the long term period (**D-F** 2050-2100), respectively.

**Table 1. Site and dataset descriptions**

Location	Elevation (m asl.)	Latitude °	Longitude °	Mean annual temperature (°C)	Minimum temperature (°C)	Absolute minimum temperature (°C)	Number of freezing events	First Frost (Autumn) DOY	Last Frost (Spring) DOY	Number of observations			
										Endodormancy Release		Budburst	
										Dataset 1 (C/V)	Dataset 2 (C/V)	Dataset 1 (C/V)	Dataset 2 (C/V)
Balandran	69	43.758	4.516	16.90	12.00	-3.78	14.5	340	50	1/1	1/1	0/0	0/0
Chatte	304	45.143	5.282	13.62	8.15	-9.39	61.7	308	102	0/0	0/0	12/11	11/12
Creysse	115	44.887	1.597	14.65	8.52	-8.50	52.4	309	104	0/0	0/0	13/12	12/13
Crouël	340	45.779	3.142	13.25	9.26	-11.51	59.6	302	108	13/12	12/13	4/4	4/4
Orcival	1150	45.683	2.842	12.92	7.72	-12.13	97.4	291	126	1/1	1/1	1/0	0/1
Terrasson	90	45.136	1.300	14.61	8.96	-9.69	47.4	311	100	1/1	1/1	1/0	0/1
Theix	945	45.706	3.021	9.70	6.22	-15.11	100.3	282	129	1/1	1/1	1/0	0/1
Toulonne	22	44.557	-0.263	15.38	10.56	-6.09	25.9	325	74	1/0	0/1	9/9	9/9

**Table 2.** Quality of the prediction of endodormancy release dates (ER) using different functions and two different calibration datasets. RMSE, RMSEP and AIC lower than 110% of the minimum RMSE or RMSEP are indicated in bold. Dates for onset of chilling accumulation ( $D_{CA}$ ) were either fixed (Julian Day) or computed according to: date of first frost (FF), minimum temperature ( $T_{min}$ ), mean temperature ( $T_{mean}$ ), photoperiod, minimum chilling unit ( $CU_{min}$ ), leaf fall using temperature (LFT) or temperature and photoperiod (LFPT) and dormancy induction state using the DORMPHOT model (DP). Ori and adj refer to the original published version (ori) or adjusted to the data (adj). Chilling effect were only positive, using the reverse Richardson function, or positive at low temperature and negative at warm temperature, using the smoothed Utah function.

Onset of chilling accumulation $D_{CA}$	Chilling effect	k	Dataset 1			Dataset 2				
			n	RMSE	RMSEP	AIC	n	RMSE	RMSEP	AIC
Julian Day	Positive only	4	18	<b>12.16</b>	11.57	<b>97.9</b>	17	8.96	<b>13.58</b>	<b>82.6</b>
	Positive & negative	6	18	<b>12.50</b>	11.49	<b>102.9</b>	17	9.51	14.26	88.6
Mean Temp	Positive only	4	18	<b>12.63</b>	11.18	<b>99.3</b>	17	9.36	<b>13.46</b>	<b>84.0</b>
	Positive & negative	6	18	13.24	11.00	<b>105.0</b>	17	10.39	19.22	91.6
Min Temp	Positive only	4	18	<b>12.64</b>	10.47	<b>99.3</b>	17	9.53	<b>13.50</b>	<b>84.7</b>
	Positive & negative	6	18	12.92	9.32	<b>104.1</b>	17	9.40	14.31	88.2
First Frost	Positive only	3	18	17.12	13.30	108.3	17	13.28	17.76	93.9
	Positive & negative	5	18	14.78	12.58	<b>106.9</b>	17	11.22	15.58	92.2
Photoperiod	Positive only	4	18	<b>12.31</b>	10.31	<b>98.4</b>	17	<b>7.80</b>	<b>13.90</b>	<b>77.8</b>
	Positive & negative	6	18	14.39	12.85	108.0	17	8.57	14.31	85.0
$CU_{min}$ ori	Positive only	3	18	15.02	12.82	<b>103.5</b>	17	11.23	16.21	88.2
	Positive & negative	1	18	44.35	47.87	138.5	17	51.32	40.07	135.9
$CU_{min}$ adj	Positive only	7	18	12.77	10.56	<b>105.7</b>	17	10.28	<b>13.36</b>	93.2
	Positive & negative	9	18	13.27	<b>8.30</b>	111.1	17	8.68	<b>13.48</b>	91.5
Leaf Fall Thermal ori	Positive only	3	18	12.88	10.30	<b>98.0</b>	17	9.21	<b>13.98</b>	<b>81.5</b>
	Positive & negative	5	18	12.83	10.12	<b>101.9</b>	17	9.11	14.19	85.1
Leaf Fall Thermal adj	Positive only	6	18	<b>11.91</b>	10.77	<b>101.2</b>	17	<b>7.79</b>	<b>13.59</b>	<b>81.8</b>
	Positive & negative	8	18	<b>11.86</b>	13.29	<b>105.0</b>	17	<b>7.75</b>	14.43	85.6
Leaf Fall Photothermal ori	Positive only	3	18	13.23	<b>8.54</b>	<b>99.0</b>	17	8.08	<b>13.98</b>	<b>77.0</b>
	Positive & negative	5	18	13.42	<b>8.99</b>	<b>103.5</b>	17	<b>7.71</b>	14.24	<b>79.4</b>
Leaf Fall Photothermal adj	Positive only	6	18	12.73	<b>8.72</b>	<b>103.6</b>	17	<b>7.86</b>	<b>14.15</b>	<b>82.1</b>
	Positive & negative	8	18	<b>12.26</b>	10.67	<b>106.2</b>	17	<b>7.64</b>	<b>14.06</b>	85.1
DORMPHOT ori	Positive only	3	18	12.77	<b>9.08</b>	<b>97.7</b>	17	8.20	<b>13.86</b>	<b>77.5</b>
	Positive & negative	5	18	13.11	9.55	<b>102.6</b>	17	8.87	14.38	<b>84.2</b>
DORMPHOT adj	Positive only	7	18	<b>11.79</b>	<b>8.45</b>	<b>102.8</b>	17	<b>7.72</b>	<b>12.90</b>	<b>83.5</b>
	Positive & negative	9	18	<b>11.51</b>	10.35	<b>105.9</b>	17	<b>7.20</b>	14.27	85.1

11

12

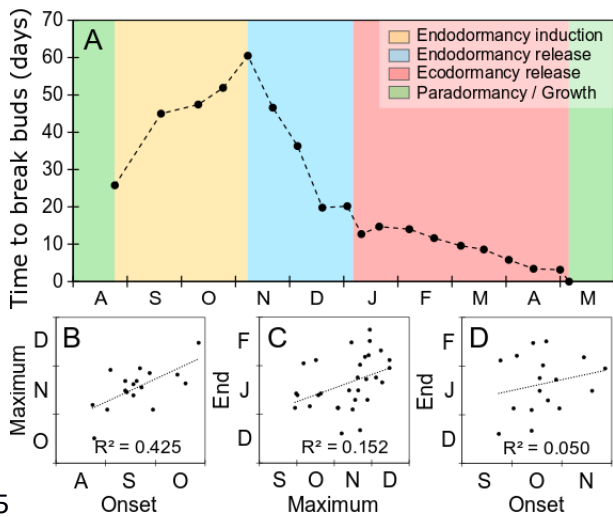
**Table 3.** Quality of the prediction of budburst dates (BB) using different functions and two different calibration datasets. RMSE, RMSEP and AIC lower than 110% of the minimum RMSE or RMSEP are indicated in bold. Dates for onset of chilling accumulation ( $D_{CA}$ ) were either fixed (Julian Day) or computed according to date of first frost (FF), minimum temperature ( $T_{min}$ ), mean temperature ( $T_{mean}$ ), photoperiod, minimum chilling unit ( $CU_{min}$ ), Leaf fall using temperature (LFT) or temperature and photoperiod (LFPT) and DORMPHOT (DP). Ori and Adj refer to the original published version (ori) or adjusted to the data (adj). Chilling effect were only positive or positive at low temperature and negative at warm temperature, using the reverse Richardson and smoothed Utah functions respectively.

Onset of chilling accumulation $D_{CA}$	Chilling effect	Dataset 1			Dataset 2					
		k	n	RMSE	RMSEP	AIC	n	RMSE	RMSEP	AIC
Julian Day	Positive only	5	41	<b>8.04</b>	<b>7.06</b>	<b>180.9</b>	39	<b>6.92</b>	<b>7.27</b>	<b>160.9</b>
	Positive & negative	7	41	8.15	<b>7.25</b>	<b>186.1</b>	39	<b>7.28</b>	7.88	<b>168.8</b>
Mean Temp	Positive only	5	41	<b>8.10</b>	<b>7.31</b>	<b>181.5</b>	39	7.69	<b>7.55</b>	<b>169.1</b>
	Positive & negative	7	41	8.63	7.86	<b>190.7</b>	39	8.86	7.89	184.1
Min Temp	Positive only	5	41	<b>7.85</b>	<b>7.21</b>	<b>178.9</b>	39	7.58	<b>7.57</b>	<b>168.0</b>
	Positive & negative	7	41	11.36	12.73	213.3	39	10.97	10.00	200.9
First Frost	Positive only	4	41	9.52	16.29	192.7	39	14.72	8.75	217.7
	Positive & negative	6	41	40.95	86.24	316.4	39	72.30	10.69	345.9
Photoperiod	Positive only	5	41	<b>8.01</b>	<b>6.74</b>	<b>180.7</b>	39	<b>6.94</b>	<b>7.32</b>	<b>161.1</b>
	Positive & negative	7	41	9.66	7.97	199.9	39	<b>7.18</b>	8.09	<b>167.8</b>
$CU_{min}$ ori	Positive only	4	41	11.17	10.88	205.9	39	9.33	9.27	182.2
	Positive & negative	2	41	54.34	63.04	331.6	39	63.84	55.42	328.2
$CU_{min}$ adj	Positive only	8	41	<b>7.94</b>	7.48	<b>185.9</b>	39	7.81	7.66	<b>176.3</b>
	Positive & negative	10	41	9.80	9.75	207.1	39	10.29	10.56	201.8
Leaf Fall Thermal ori	Positive only	4	41	<b>7.67</b>	<b>6.88</b>	<b>175.0</b>	39	7.66	7.70	<b>166.8</b>
	Positive & negative	6	41	<b>7.75</b>	<b>6.76</b>	<b>179.9</b>	39	<b>7.36</b>	<b>7.41</b>	<b>167.7</b>
Leaf Fall Thermal adj	Positive only	7	41	8.30	<b>6.77</b>	<b>187.6</b>	39	<b>6.84</b>	<b>7.29</b>	<b>163.9</b>
	Positive & negative	9	41	8.31	7.71	<b>191.6</b>	39	<b>6.92</b>	<b>7.42</b>	<b>168.9</b>
Leaf Fall Photothermal ori	Positive only	4	41	<b>7.82</b>	<b>7.16</b>	<b>176.6</b>	39	<b>7.08</b>	<b>7.37</b>	<b>160.7</b>
	Positive & negative	6	41	<b>7.47</b>	<b>6.68</b>	<b>176.9</b>	39	<b>7.01</b>	<b>7.18</b>	<b>163.9</b>
Leaf Fall Photothermal adj	Positive only	7	41	<b>7.49</b>	<b>6.82</b>	<b>179.1</b>	39	<b>6.97</b>	<b>7.23</b>	<b>165.4</b>
	Positive & negative	9	41	80.49	73.53	377.8	39	<b>7.14</b>	<b>6.94</b>	<b>171.3</b>
DORMPHOT ori	Positive only	4	41	<b>7.74</b>	<b>6.89</b>	<b>175.9</b>	39	<b>7.13</b>	<b>7.63</b>	<b>161.3</b>
	Positive & negative	6	41	<b>7.39</b>	<b>6.82</b>	<b>176.0</b>	39	<b>7.05</b>	<b>7.51</b>	<b>164.4</b>
DORMPHOT adj	Positive only	8	41	<b>7.67</b>	<b>6.90</b>	<b>183.1</b>	39	<b>7.28</b>	<b>7.67</b>	<b>170.9</b>
	Positive & negative	10	41	8.88	<b>7.04</b>	199.1	39	<b>7.00</b>	8.23	<b>171.8</b>

22

23

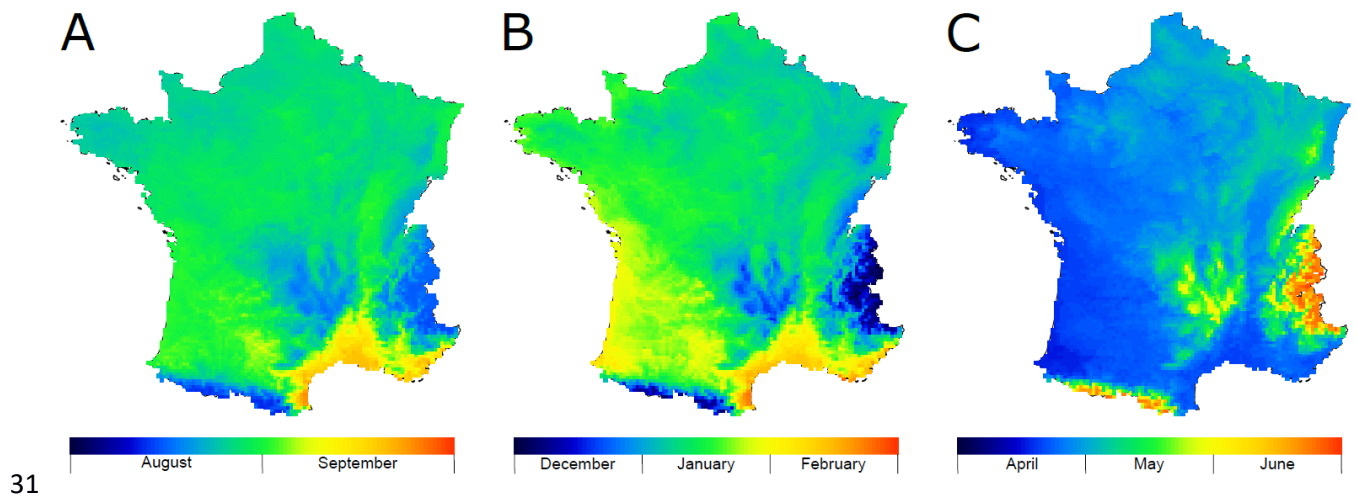
24



25

26 **Figure 1. A.** Time to break buds under forcing conditions for one node cuttings of *Juglans*  
 27 *regia* cv Franquette. Different colors represent the different phenological stages based on  
 28 the dynamics in time to break buds. **B-D.** Correlations between the onset of endodormancy  
 29 induction, the maximum endodormancy depth and endodormancy release.

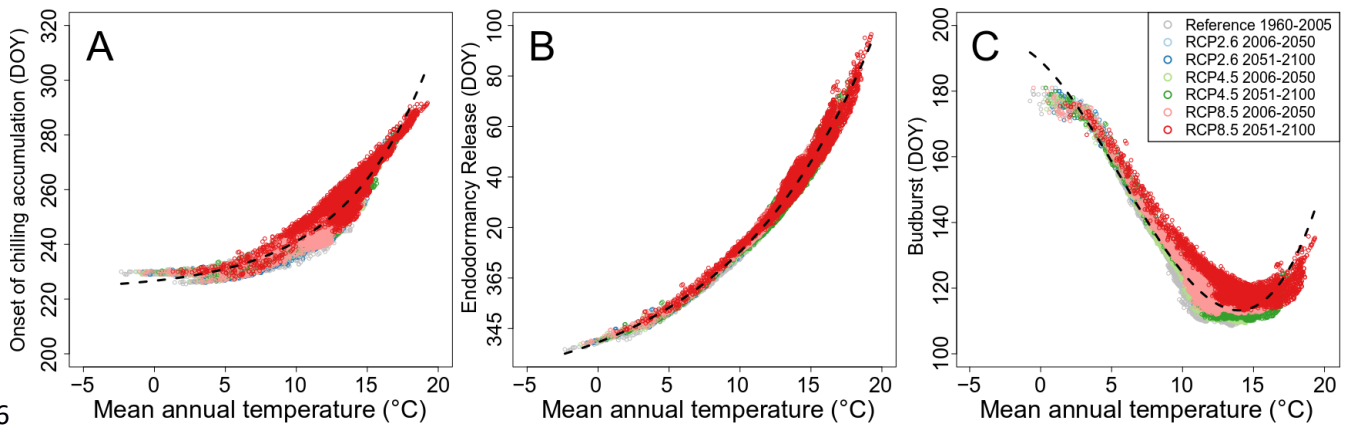
30



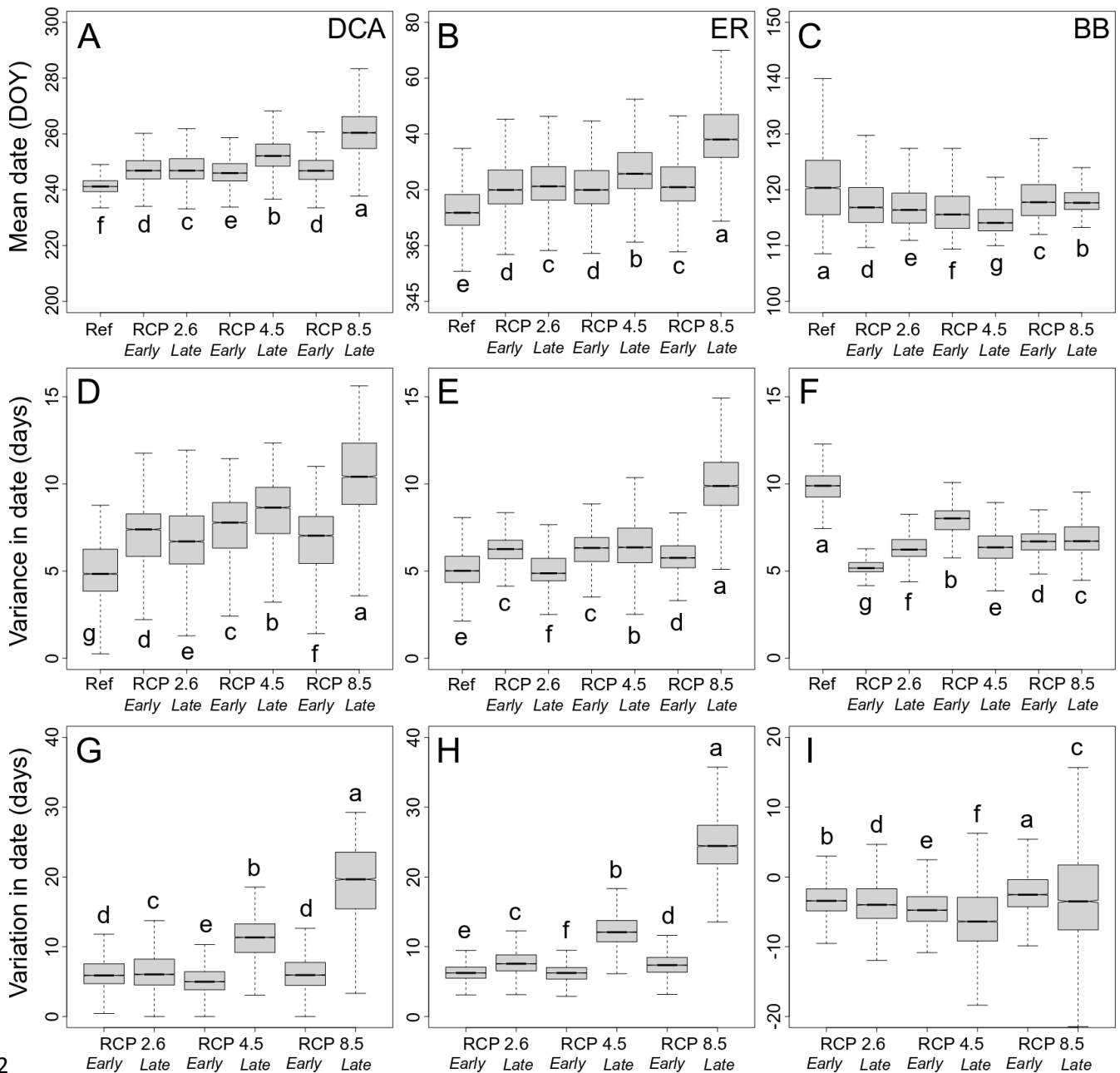
31

32 **Figure 2.** Average dates of onset of chilling accumulation (A), endodormancy release (B)  
 33 and budburst (C) predicted across France under current climatic conditions.

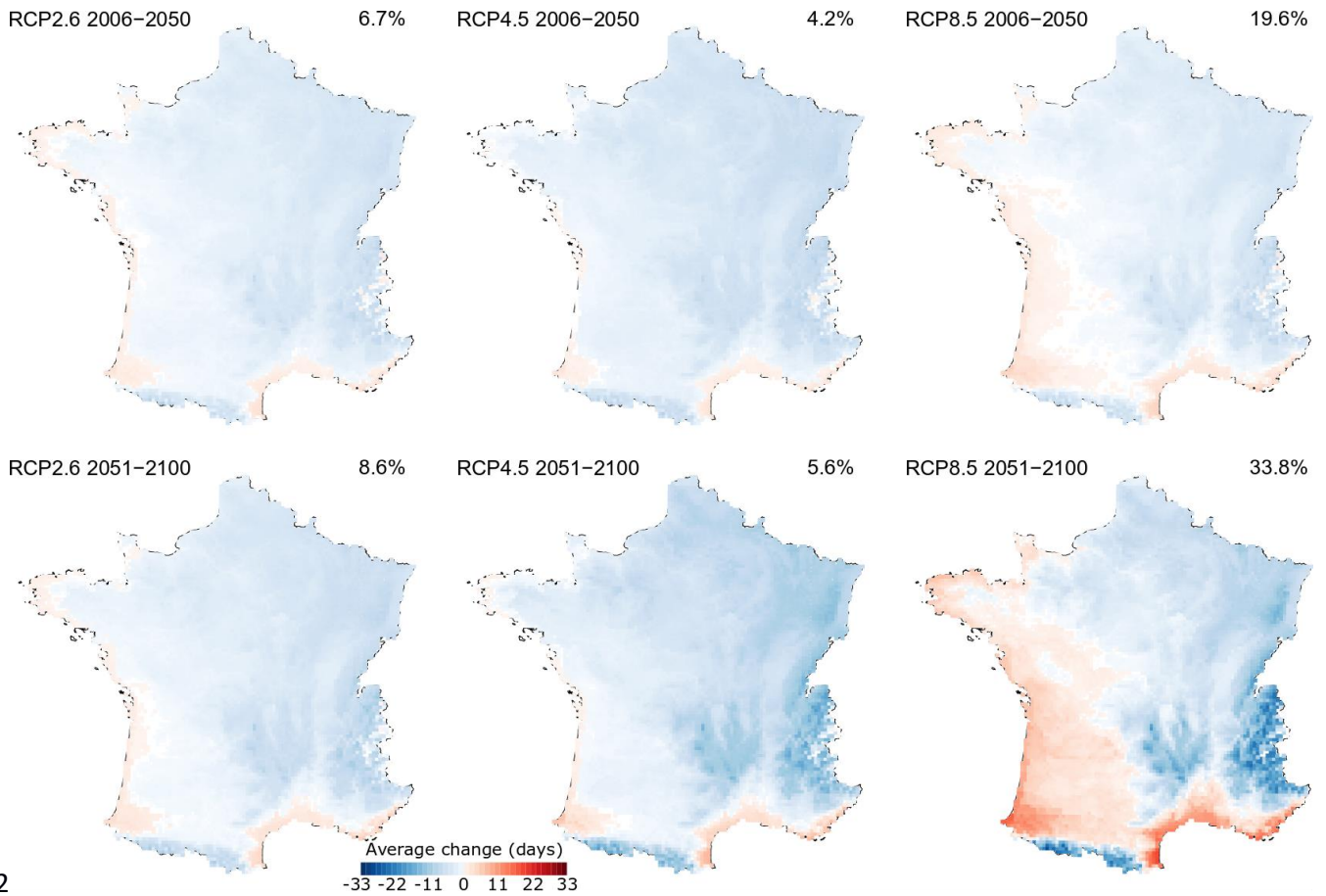
34



36  
 37 **Figure 3. A-C.** Average date of onset of chilling accumulation (A), endodormancy release  
 38 (B) and budburst (C) depending on mean annual temperature across France under different  
 39 climatic *scenarii*. Exponential (A, B) and cubic (C) functions were represented in black  
 40 dashed lines.



42 **Figure 4 A-C** Distribution of the mean (A-C) and variance (D-E) in the date of onset of 44chilling accumulation (A, D), endodormancy release (B, E) and budburst (C, F) in the 45current period (Ref) or RCP scenario in the early (2006-2050) and late part of the XXI 46century (2051-2100) in France. **G-I** Distribution of the variation compared to the reference 47period in the mean date of onset of chilling accumulation (G), endodormancy release (H) 48and budburst (I). The box represents the upper and lower quartile with the median indicated 49by a thick black line, the whiskers represents the 1<sup>st</sup> and 9<sup>th</sup> decile, outliers were not 50represented. Different letters indicate a significantly different distribution across scenario 51according to the non-parametric Kruskal Wallis test.



52

53 **Figure 5.** Relative change compared to the present period in average budburst dates  
54 across France according to different climatic *scenarii* (RCP2.6, RCP4.5 and RCP 8.5) and  
55 time periods (2006-2050 and 2051-2100). Earlier and later budburst dates than the current  
56 climate are represented in blue and red, respectively.